AD-A052 251 RHODE ISLAND UNIV KINGSTON DEPT OF ELECTRICAL ENGIN--ETC F/G 20/1
A DEEP WATER MODEL OF THE FLOODED CYLINDRICAL RADIATOR.(U)
MAY 63 R S HAAS, F H MIDDLETON NONR-396(12)

UNCLASSIFIED TR-1 NL

| OF |
AD
A052 251

END
DATE FILMED
5-78
DDC

DIVISION OF ENGINEERING RESEARCH AND DEVELOPMENT

DEPARTMENT OF ELECTRICAL ENGINEERING

A Deep-Water Model of the Flooded Cylindrical Radiator

by F. H. MIDDLETON and R. S. HASS

Contract No. Nonr-396(12)
Technical Report No. 1

Prepared for
ACOUSTICS PROGRAMS
Naval Applications Group
Office of Naval Research

UNIVERSITY OF RHODE ISLAND
KINGSTON, RHODE ISLAND

(6)

A DEEP WATER MODEL OF THE FLOODED CYLINDRICAL RADIATOR.

(9) Technical rept.,

by

(10) Robert S. Haas
and
Foster H. Middleton

Department of Electrical Engineering
University of Rhode Island
Kingston, Rhode Island

(15) Contract No. Nonr-396(12)

(11) May 63 (14) TR-1

(12) 2pp.

Prepared for:

Office of Naval Research
Acoustics Programs

I. Introduction

This work was undertaken to learn reasons for the behavior of the "barrel-stave" acoustic radiator, operating in a condition devoid of all pressure release. This source configuration is most difficult to deal with because it has a shape which is mathematically awkward. It's height is small in comparison with the diameter, thus making cylindrical coordinates of little value. Admittedly, the cylindrical radiator does not closely approximate a sphere, but a circumscribing sphere (radius the same as the source radius) has distinct advantages. The radiation from a spherical source with an arbitrary surface velocity distribution is easily handled analytically. It is this fact that makes the present approach attractive. Also, some computer results provide plausible explanations for unexpected phenomena that occur in tests with these radiators.

In the interest of completeness, the theory of the spherical radiator will be presented. Applications of this theory to the special problem at hand indicate what can be expected from the method. Consideration of different frequencies and different velocity distributions provide conclusions that are very useful in the basic design process and in the process of modifying the performance of existing designs.

II. The Theory of Radiation From a General Spherical Source

The general solution of a spherical radiator can be found in several references, (1), (2), (3), For the application at hand, it will be derived in more detail to unify the analytic procedure and symbols.

Let a spherical radiator with radius, a, be immersed in an infinite, isotropic and homogeneous fluid of density ρ and sound velocity c. The acoustic field outside the radiator can be expressed by a scalar wave equation in spherical coordinates, where ψ is the velocity potential, and $k = \omega/c$.

$$\frac{1}{c^2}\frac{\partial^2\psi}{\partial t^2} = r^2\frac{\partial^2\psi}{\partial r^2} + \frac{1}{\sin\theta}\frac{\partial}{\partial\theta}\left[\sin\theta\frac{\partial\psi}{\partial\theta}\right] + \frac{1}{\sin^2\theta}\frac{\partial^2\psi}{\partial\phi^2} + k^2\psi \qquad (1)$$

If there is no velocity potential variation with the angle ϕ (which corresponds to the breathing radial mode of the cylindrical radiator), then eq. (1) can be simplified to the two dimensional case.

$$\frac{1}{c^2}\frac{\partial^2\psi}{\partial t^2} = r^2\frac{\partial^2\psi}{\partial r^2} + \frac{1}{\sin\theta}\frac{\partial}{\partial\theta}\left[\sin\theta\frac{\partial\psi}{\partial\theta}\right] + k^2\psi \qquad (2)$$

The solution of this equation is well known and can be easily found to be:

$$\psi = \sum_{m=0}^{\infty} A_m P_m(\cos\theta)\left[j_m(kr) + in_m(kr)\right] e^{-i\omega t} \qquad (3)$$

A_m are constants to be determined by the boundary conditions. The quantities $P_m(\cos\theta)$, $j_m(kr)$, and $n_m(kr)$ are Legendre polynomials, spherical Bessel functions, and spherical Neumann functions respectively.

Since the radial component of velocity is the radial derivative of the velocity potential:

$$U_r(r,\theta) = \frac{\partial \psi}{\partial r} = k\frac{\partial \psi}{\partial (kr)} = \sum_{m=0}^{\infty} A_m P_m(\cos\theta) k[j_m'(kr) + in_m'(kr)] e^{-i\omega t} \qquad (4)$$

A given velocity distribution on the surface of the spherical radiator such as $U(a,\theta)e^{-i\omega t}$ can be expanded in terms of a series of Legendre functions of the form:

$$U(a,\theta)\, e^{-i\omega t} = \sum_{m=0}^{\infty} U_m P_m(\cos\theta)\, e^{-i\omega t} \qquad (5)$$

with

$$U_m(a,\theta) = (m + \tfrac{1}{2}) \int_{\alpha}^{\beta} U(a,\theta) P_m(\cos\theta) \sin\theta \, d\theta \qquad (6)$$

Where m is an integer and α and β are the values of θ between which the active surface exists.

When r equals a, eq. (4) should meet the boundary condition of eq. (5). By equating them,

$$A_m(a,\theta) = \frac{U_m}{k[j_m'(ka) + in_m'(ka)]} \qquad (7)$$

From the results of eqs. (3), (7), the following acoustic field parameters can be obtained.

The resulting outgoing pressure wave will be:

$$p = \rho \frac{\partial \psi}{\partial t} = -i\omega\rho\psi = -i\omega\rho \sum_{m=0}^{\infty} A_m P_m(\cos\theta)[j_m(kr) + in_m(kr)] e^{-i\omega t} \qquad (8)$$

and the acoustic impedance may be expressed as:

$$Z_r = \iint \frac{p}{u_r} ds = \int_0^{\pi} \frac{p 2\pi r^2 \sin\theta}{u_r} d\theta$$

$$= \int_0^{\pi} \frac{-i\omega\rho \sum_{m=0}^{\infty} A_m P_m(\cos\theta)[j_m(kr) + in_m(kr)]2\pi r^2 \sin\theta \, d\theta\theta}{\sum_{m=0}^{\infty} A_m P_m(\cos\theta)\, k[j_m'(kr) + in_m'(kr)]}^4 \quad (9)$$

$$Z_r = i2\pi r^2 \rho c \int_0^{\pi} \frac{\sum_{m=0}^{\infty} A_m P_m(\cos\theta)[j_m(kr) + in_m(kr)] \, d(\cos\theta)}{\sum_{m=0}^{\infty} A_m P_m(\cos\theta)[j_m'(kr) + in_m'(kr)]} \quad (10)$$

The acoustic impedance presented to the radiator can be obtained by setting r = a in equation (10).

Based on the equations (4), (8), and (10), other acoustic field quantities such as intensity and radiated power can be found. The intensity is given by the real part of the product $\frac{1}{2} p^* u_a$ (where p^* is the complex conjugate of p). The radiated power is determined by integrating the intensity over a closed surface. At the present, however, interest will be centered on the development of a computer program which will ~~be centered on the development of a computer program which will~~ calculate the far field pressure pattern of the short cylinder.

III The Program

The last equation (8) for pressure is the one that has been programmed for computer solution. An effort was made to make the computation time small so that excessive computer time would not be necessary. It is not the ultimate in compactness and spped as it might have been had it be deribed for a solution to one specific problem. It has been deliberately made as general as possible within the confines of the problem that was initially specified. It contains, for example, numerous sense switch

settings enabling the user to check the progress and accuracy of a solution at many points within the body of the main program. Instructions for additional computations can easily be inserted.

The program has restrictions, of course, but they do not in any way impede its intended use. All of the limits and restrictions, which are summarized later in this report, can be easily increased to permit investigation of surface velocity distributions of greater complexity than those thus far attempted.

Analysis of Results

I. In analyzing the computer produced pressure patterns it is necessary to keep in mind that a spherical coordinate system was employed in the development. Consequently, the analysis will be in terms of an equivalent circumscribed spherical radiator.

The actual cylindrical radiator which provided the experimental data was approximately four feet in diameter and had an active axial length of approximately twenty inches. The circumscribed sphere was arbitrarily established as having a two foot radius.

The patterns produced many interesting and not altogether unexpected results from which certain interpretations and conclusions will be drawn.

It is to be noted that in describing any surface velocity distribution in terms of Legendre polynomials, the closeness of "fit" depends largely upon the physical size of the sphere relative to the operating wavelength. For this purpose the parameter (ka) is used in which (a) is the radius of the sphere.

$$ka = \left(\frac{2\pi}{\lambda}\right)a = 2\pi\left(\frac{a}{\lambda}\right) = \frac{\text{circumference}}{\text{wavelength}}$$

The sphere is a geometric shape with many possible modes of vibration. These modes, or resonances, determine to a large extent the magnitudes of the various Legendre terms. In other words, a Legendre term containing a frequency term whose wavelength fits the critical dimension of the sphere will be enhanced whereas a term which does not fit as well will be diminished. Certain terms may be rejected altogether if the sphere presents to them an anti-resonance. In most cases this results from the nature of the driving disturbance, a completely even symmetry in the velocity distribution giving rise to only even order Legendre terms and a completely odd

source distribution giving rise to only odd terms. Symmetry in this sense refers to symmetry about the equator or about the angular position $\theta = \frac{\pi}{2}$.

In the following discussion a $\frac{1}{2}\lambda$ resonance refers to that condition of operation which the circumference of the sphere is one wavelength, or ka=1. Similarly, a $\frac{3}{2}\lambda$ resonance implies that ka=3. For the values of ka less than 1, the predominant Legendre term is P_o, which is a constant independent of the polar angle. This term characterizes the behavior of the sphere (or other shapes) at extremely low frequencies for which $ka << 1$. Since a given Legendre polynomial contains components of all lower order terms possessing the same symmetry no pattern is the result of a single term with the exception of the P_o and P_1 polynomials which contain only one term each. Operation at exactly one of the resonance modes, however, does produce patterns which are controlled essentially by a predominant single term.

In selecting velocity distributions it is to be noted that segments of constant amplitude were employed. This was done for several reasons. The computer program is simplified in that portion which evaluates the coefficients, A_m, from the velocity distribution. In addition, the "filtering effect" of the sphere resonances causes in general, the lower order terms of the Legendre polynomials to predominate in determining the far field pressure effects. In other words, the idealized distribution shown in fig. 1 can contribute primarily those components which coincide with the first few modes as determined by ka.

II. It can be seen in fig. 1 that with the velocity distribution given and with ka=1 that the dominant mode of operation is predetermined by the even symmetry of the velocity function to consist of even order Legendre polynomials only. The symmetry, as mentioned previously, is referred to an acoustic axis taken at polar angle $\theta = \frac{\pi}{2}$.

This driving mode is then a radial motion of a belt around the sphere between the polar angles $\frac{\pi}{3}$ and $\frac{2\pi}{3}$ radians. It is to be noted that although the sphere is in resonance in the $\frac{1}{2}\lambda$ mode, no output is observed due to this mode since the $\frac{1}{2}\lambda$ resonance must be excited by an odd symmetric velocity function.

The nearest acceptable modes are the P_o and the P_2. The pattern due to the P_o would be a circle, and with respect to a circle drawn in for comparison, the effects of a slight $\frac{2}{2}$ (λ) (two halves lambda) mode can be seen. The coefficients A_m, of the Legendre terms are determined principally by the $(j_m'(ka) + i\, n_m'(ka))$ in the denominator of the A_m expression. Since the spherical Bessel derivatives increase rapidly with the order m for small argument, ka, the higher order terms in A_m disappear equally rapidly. Therefore, for the pattern under discussion the only terms of significance are the P_o and the P_2. In other words, the sphere tends to breathe as a unit and the resulting far field pressure is quite uniform as a function of the polar angle. As (ka) is increased the effect of the next higher order mode, P_4, is observed. Due to the effect of the $[j_n(kr)+in_m(kr)]$ term the far field approximation causes each succeeding Legendre term to be of alternate sign, i.e. the terms add as $P_o - P_2 + P_4 - P_6$ etc. Since this series of terms is convergent, however, each succeeding term generally contributes less than its predecessors with the important exception of resonant operation. In the cases studied with (ka) up to 4.5 and with either pure even or pure odd excitations the pattern can be interpreted reasonably well by observing notch locations and relative lobe strengths and comparing these with hand sketches of various Legendre combinations.

The first interesting departure from the pure breathing mode of operation, which incidentally implied rigid caps, allows the polar caps

to move such that a constant volume is maintained. The pattern characteristically assumes the form of fig. 6 and 7 with a sharply defined notch. Any pattern with deep notches cannot contain the P_o term in any appreciable amplitude. Since the excitation is still of even symmetry, the first allowable term is P_2, but with ka=1 for this figure there can be little output so far from the resonance mode (or ka=2).

The normal convergence of the coefficients at ka=1 precludes any significant output at any higher mode, hence the pattern is almost a pure P_2 but of very low amplitude. Increasing (ka) to 2.5 shows essentially the same content, but at a higher output level. Actually at ka=2.5 the resonance point for the $\frac{2}{2}\lambda$ mode has been passed. This occurred at ka=2 and would have yielded a maximum output if operated at the corresponding frequency.

The next significant patterns occur whenever an odd mode of excitation is employed, see fig. 8 and 10. In this mode there will always be a complete notch along the active or acoustic axis. With odd excitation, however, the Legendre terms will be restricted to the odd orders. The lowest odd order is the P_1 which would be in resonance at ka=1 corresponding to the $\frac{1}{2}\lambda$ mode. A resonance pressure pattern at ka=1 would be almost a dipole pattern with the major radiation occurring along the polar axis. The actual barrel stave transducer to which reference has been made previously is built in two identical sections so that there are in reality two active bands of barrel staves adjacent to each other. The results of the pattern of fig. 8 indicate that instead of driving the two section in phase, as has been customary, opposite phased excitation would give rise to a strong dipole pattern vertically oriented. The actual (ka) used in the patterns of fig. 8 was 2.5, hence the appearance of a small P_3 component. The pure

dipole pattern is drawn for comparison, and it can be seen that at ka=2.5 the output is essentially "dipole like".

The excitation function for fig. 10 is for a double reversal of velocity along the active length and the "filtering" action of the sphere maintains essentially the same Legendre content until ka $\approx$ 5 where further notching will appear.

It is postulated here that the velocity distribution of figures 8, 9, and 10 are possible if, at certain critical frequencies, a flexural standing wave exists along the length of the stave. If so, this would give rise to the patterns of the above mentioned figures depending upon the boundary conditions. The velocity distribution of figure 9 is that of figure 8 phase shifted along the length of the stave. The excitation for the pattern of figure 9 is therefore even symmetric of the P_2 type principally, but with a reduced output along the acoustic axis. This is comparable to fig. 12 redrawn from test data. This obviously is a P_2 primary excitation with some P_4 superimposed.

Particular attention should be drawn to the pattern of figure 9, which suggests that a flexural wave might be the cause of sudden reductions in acoustic axis output at a particular frequency. This form of flexural wave could exist if the flexural wave velocity were in the neighborhood of 2000 ft/sec. Operation at a (ka) value of 2 would seem to produce a reasonable expectation of this mode of operation.

Preliminary tests on a single stave indicate a flexural wave velocity in the right order of magnitude. At the moment, however, the prime concern is the interpretation of pressure patterns on the basis of assumed velocity distributions and not on the detailed reasoning for the existance of such distributions.

One combination of breathing mode and a superimposed flexural wave has been included in this report, see fig. 11. It indicates a simple addition of the individual patterns. Other combinations immediately come to mind and some of these are currently under study and will be reported at a later date.

Conclusions

1. The spherical approach to the cylindrical radiator seems reasonable in so far as it has been applied to specific pressure patterns of an axially short cylinder.
2. To produce a breathing mode of any significant value requires that the real or assumed velocity distribution have an average value over the spherical surface.
3. Spherical resonances appear to control the pattern shape which, for the usual range of ka values, are dictated by a relatively few low order modes.
4. The existence of a flexural mode will explain certain pattern notches or other sudden reductions in acoustic output along a particular axis.
5. Multi-section transducers could be phased to produce changes in directivity such as the dipole effect discussed previously.
6. Probable surface velocities can be ascertained by observation of the far field pressure pattern.
7. The influence of volume effects on the pressure pattern can be observed.

Many workers in the field of design of large radiators have used similar mathematical approaches to a model of a short pressure equalized cylinder. Some of these seem much more appropriate than does a circumscribed sphere. One such is the prolate spheroidal coordinate system. The real justification for the spherical model is two-fold, however. The associated mathematics is vastly simpler on the one hand, and there are only very minor differences between the corresponding source distributions. That is, the sphere and the prolate spheroid are so similar and so close to each other, that only

minor differences in particle velocity are possible.

Clearly, these advantages of the sphere may be lost when the height to diameter ratio excedes unity. But when it is appropriate, the spherical model makes possible an appreciation of the individual contributions of various structural modes to the net radiation and radiation impedance effects. Knowing what the individual modal contributions are makes it possible to enhance or suppress certain ones so as to modify the acoustic properties of a specific design.

Finally, it may be said that the present design approach is an over-simplification which is warranted because of the insight it provides, even though the quantitative results are inherently inaccurate. The computer results so far have provided logical reasons for the appearance of notches in the frequency response curves and the effect of rigid sections in the polar cap regions (top and bottom) of the cylindrical transducer.

This work was undertaken with the financial support of the Martin-Marietta Corporation, Baltimore, Maryland. Present work is supported by the Acoustics Branch, Office of Naval Research.

FAR FIELD PRESSURE PATTERNS

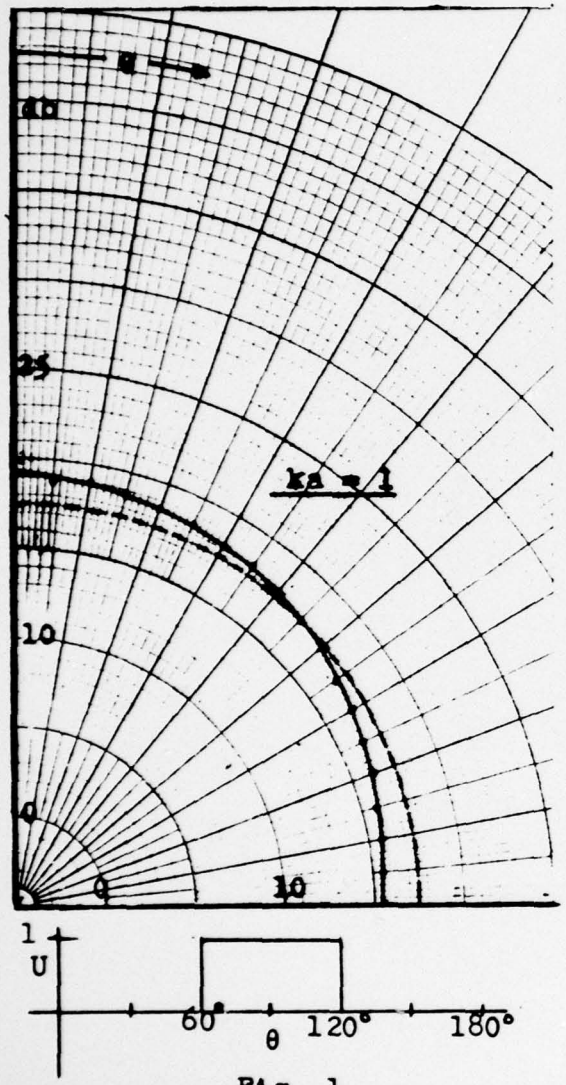

Fig. 1

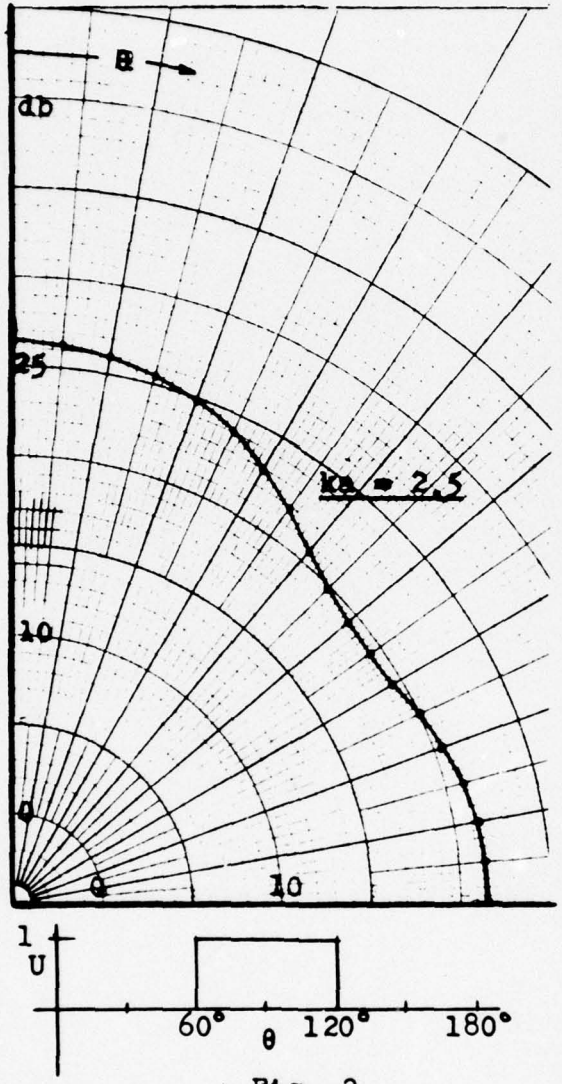

Fig. 2

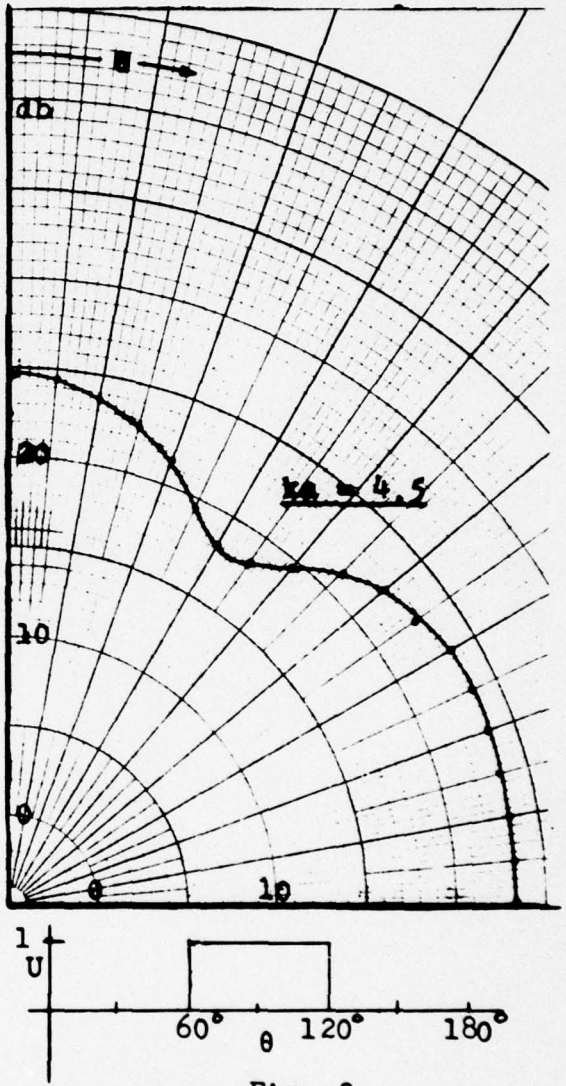

Fig. 3

FAR FIELD PRESSURE PATTERNS

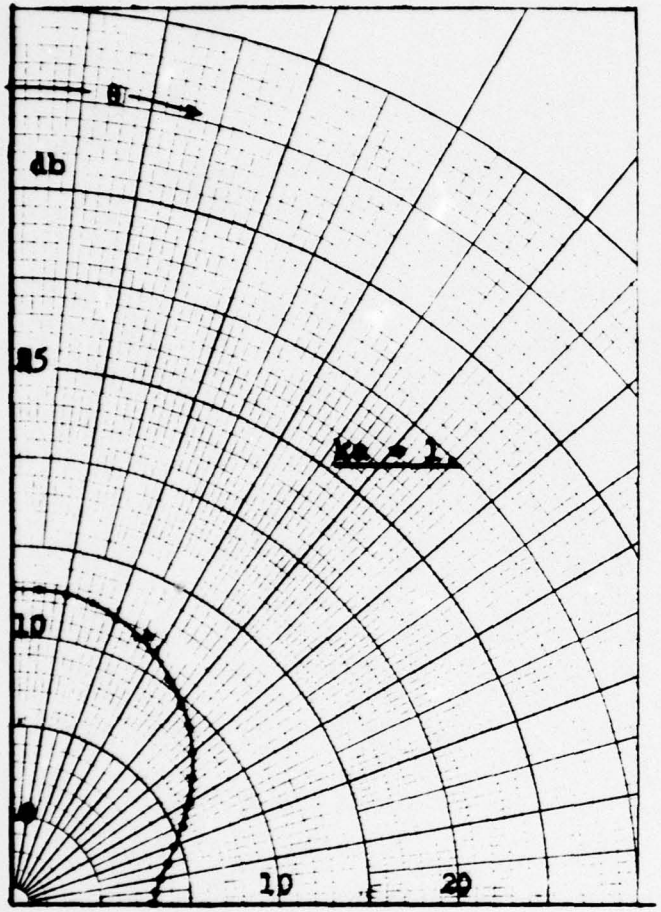

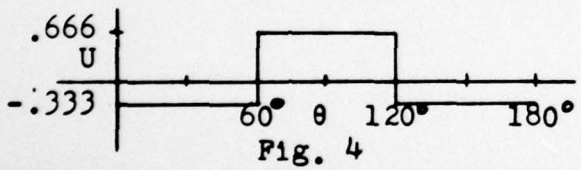

Fig. 4

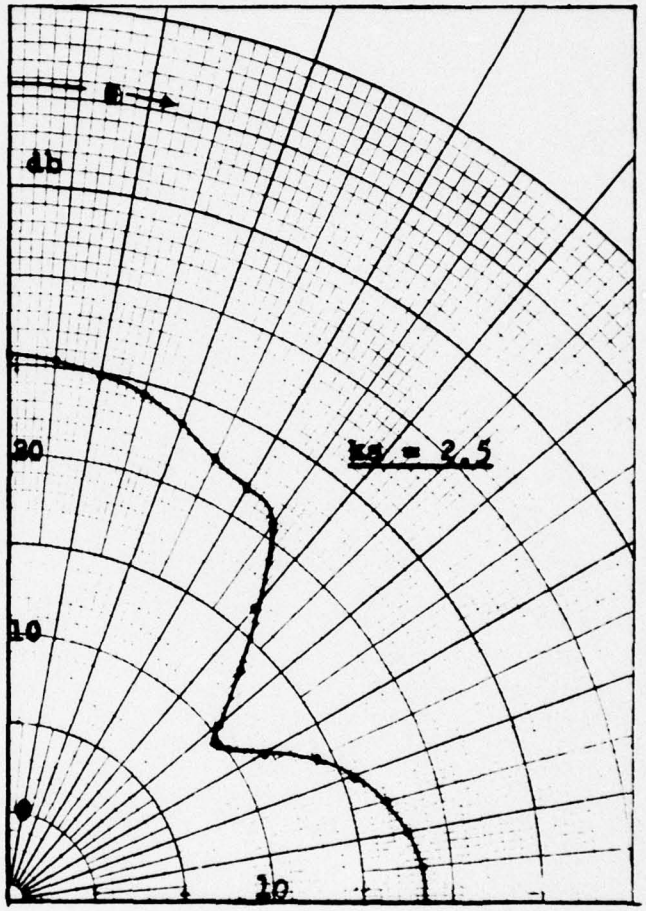

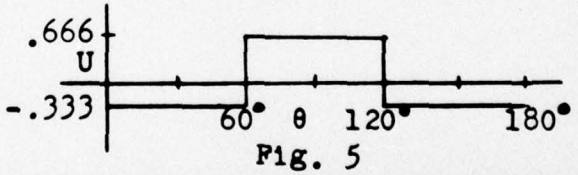

Fig. 5

FAR FIELD PRESSURE PATTERNS

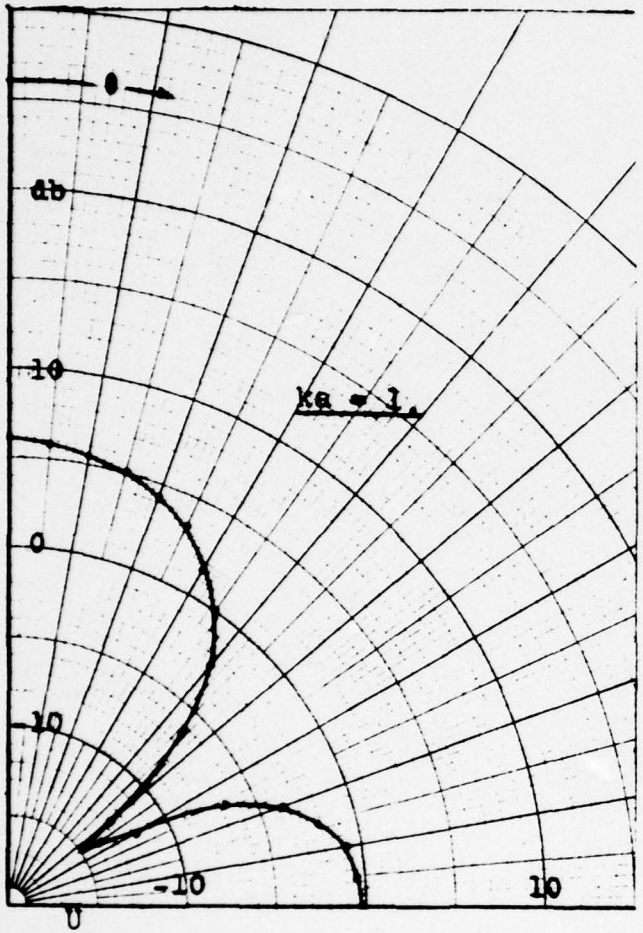

Fig. 6

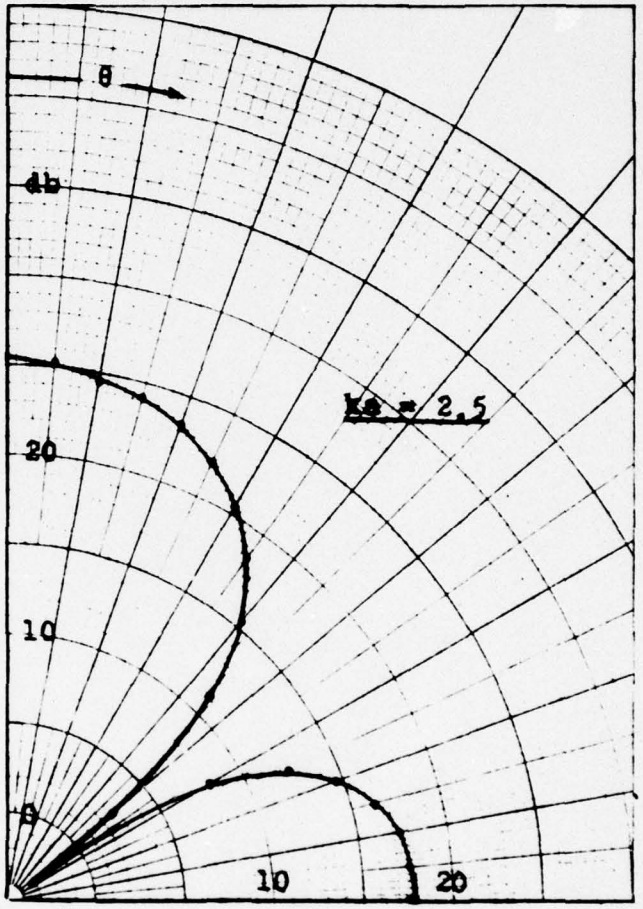

Fig. 7

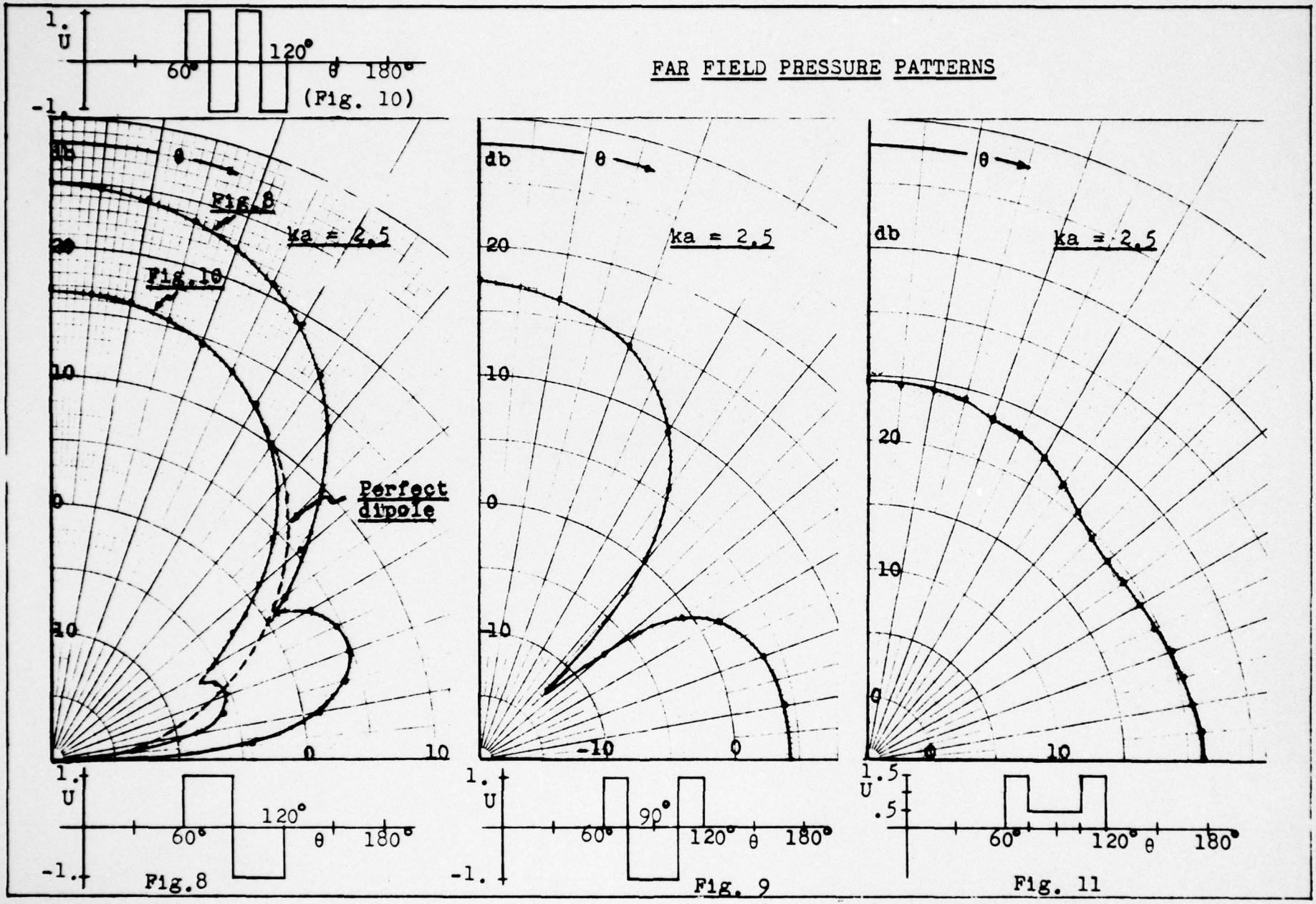
FAR FIELD PRESSURE PATTERNS
1.
U
60°
120°
θ
180°
-1.
(Fig. 10)
db
θ
Fig. 8
ka = 2.5
Fig. 10
Perfect dipole
20
10
0
10
1.
U
60°
120°
θ
180°
-1.
Fig. 8
db
θ
ka = 2.5
20
10
0
-10
1.
U
60°
90°
120°
θ
180°
-1.
Fig. 9
db
θ
ka = 2.5
20
10
0
10
1.5
U
.5
60°
120°
θ
180°
Fig. 11

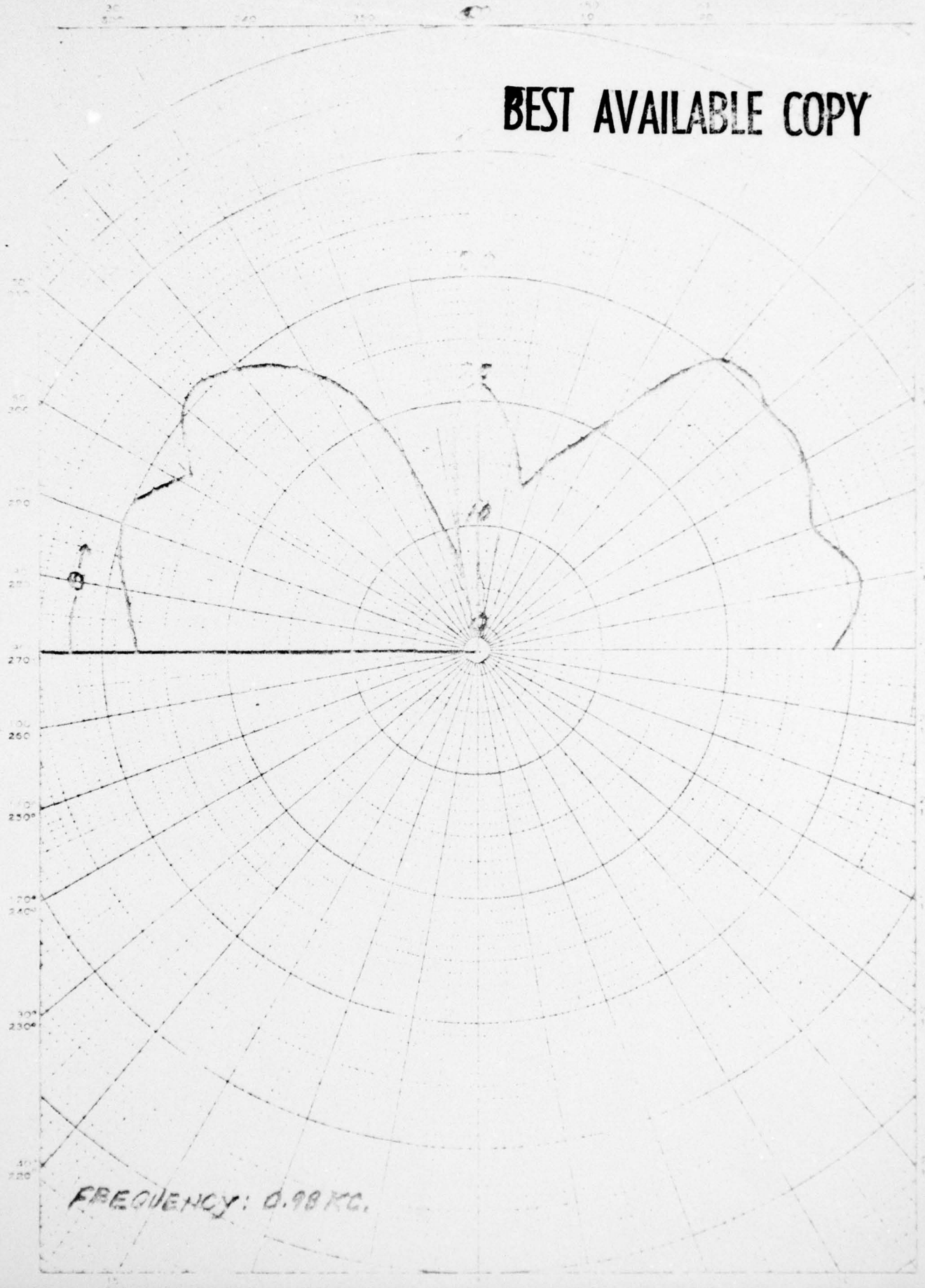

U. of Rhode Island. Dept. of Elec. Eng. A deep water model of the flooded cylindrical radiator. Tech. Report no. 1.

Name Date

Saunders 3/25/68